M-shell x-ray spectra of laser-produced gold plasmas

K. Honda and K. Mima
Institute of Laser Engineering, Osaka University, Yamadaoka 2-6, Suita, Osaka 565, Japan

F. Koike
Physics Laboratory, School of Medicine, Kitasato University, Kitasato 1-15-1, Sagamihara, Kanagawa 228, Japan

(Received 27 March 1996)

X-ray spectra of laser-produced highly charged gold-ion plasma have been studied theoretically. Energies and oscillator strengths for $3d$-$4f$ transitions are calculated in detail for nickel, copper, zinc, or galliumlike ions with a couple of spectator electrons. Based on a precise nonempirical multiconfiguration Dirac-Fock calculation, a model that could be called the noninteracting spectator-electron model (NISEM) is proposed to analyze x-ray radiation from plasmas. The NISEM extrapolates the satellite emission spectra of ions with a single spectator electron to those ions with an arbitrary number of spectator electrons. In the framework of NISEM and local thermodynamic equilibrium, the experimental spectra have been reproduced reasonably well by the present theory. [S1063-651X(97)00402-9]

PACS number(s): 52.25.Nr, 52.40.Nk, 32.70.Jz

I. INTRODUCTION

Laser-produced high-Z plasmas consist of multiply ionized ions, and a highly charged heavy ion accepts many electrons in its high-lying loosely bound orbitals. In Fig. 1, a schematic drawing is given for such a situation in nickel-like gold ions with a few spectator electrons in Rydberg orbitals. Complicated atomic and radiation processes occur in the high-Z plasmas and have been investigated extensively by the authors of Refs. [1–4]. The x-ray line spectra of highly ionized high-Z ions in laser-produced plasmas have shown the prominence of M-shell transitions of nickel, copper, zinc, and galliumlike ions. For example, in a gold plasma, x-ray line spectra of M-shell transitions in the wavelength range from 4.2 to 5.4 Å are important. Typical experimental spectra of M-shell x-ray lines of gold plasma are shown in Fig. 2. The spectra in this range were studied in detail by Bauche-Arnoult *et al.* [5]. Busquet *et al.* have also analyzed the gold spectra in a similar energy range [6]. They have introduced a broad speculative red wing in order to reproduce the spectra in the presence of densely distributed unresolvable satellite lines.

When the number of bound electrons becomes large, the line spectra may become very densely crowded. By taking advantage of this property, an approximation called the unresolved transition array (UTA) was proposed by Bauche-Arnoult *et al.* [7–10]. UTA is an effective and useful tool for spectral analysis of high-Z plasmas. An interesting extension of the UTA theory to reduce the number of UTAs for complex cases was made by Bar-Shalom *et al.*, who introduced the approximation called supertransition array (STA) [11]. In the limit of no term splitting, the STA reduces to the average atom model (AA) [12]. The UTA and/or STA models are powerful and reduce computation time significantly. These models give energy distributions, but the determination of the exact energies of a transition array is not the objective of the models. To calculate the exact energy of the transition array, we have to use a detailed calculation code. Once the exact energy of the transition array is calculated with a detailed calculation code, the energy distribution is normally obtained simultaneously. Thanks to the recent progress of computer technology, we are nowadays able to calculate both the energies and the distributions of complicated transition arrays using a detailed calculation code. However, it is still very difficult even for a present day computer to calculate the huge number of line spectra of high-Z ions with many spectator electrons. Therefore, we introduce an approximation which is closely related to the detailed calculation results.

In the present paper, we carry out a line by line calculation which enables us to evaluate the x-ray spectral profiles for an arbitrary spectator electron population [13]. We use a computer program called the general purpose relativistic atomic structure program 2 (GRASP2) [14,15] for our atomic structure calculations. The program allows us to include several open shells and to include thousands of configuration state functions (CSFs) in the calculation. Furthermore, in order to simplify the calculation, we introduce an extrapolation model which we call the noninteracting spectator-electron

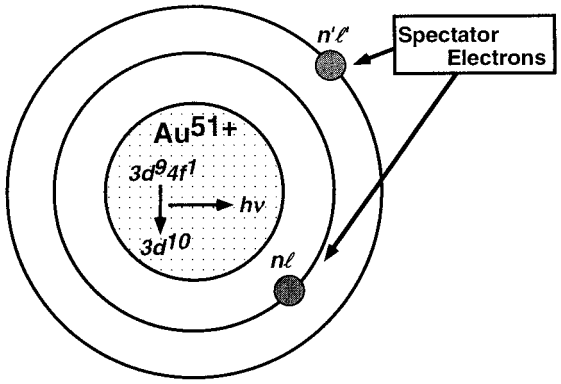

FIG. 1. Schematic drawing of a nickel-like gold ion with a few extra spectator electrons in Rydberg orbitals. For example, the energies of the $3d$-$4f$ transitions in the nickel-like ion core are modified by the presence of the spectator electrons.

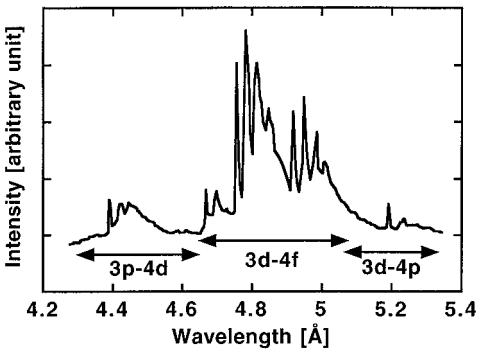

FIG. 2. Densitometer tracing of the gold spectrum from laser-produced plasma in the wavelength range: 4.2–5.4 Å. The spectrum consists mainly of $3d$-$4f$ transitions of cobalt, nickel, copper, zinc, and galliumlike ions [5].

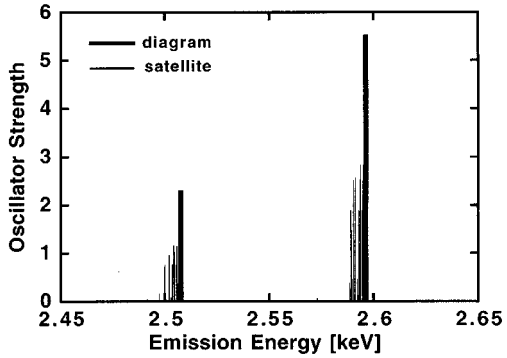

FIG. 3. Oscillator strength distribution of nd^1 spectator electron satellites for transitions:
$Au^{50+}\ 1s^2 2s^2 2p^6 3s^2 3p^6 3d^9 4f^1 nd^1 (n=5,6,7)$
$\rightarrow Au^{50+}\ 1s^2 2s^2 2p^6 3s^2 3p^6 3d^{10} nd^1$.
The $3d$-$4f$ diagram lines are also presented for comparison as thick bars.

model (NISEM). In the UTA and the STA line positions are calculated by using perturbation theory [7,11] for the case of many-spectator electrons. However, the perturbation method is in general not always justifiable even if the method yields reasonable results in comparison with the experimental results. In this paper, we confirm the validity of our approximation method NISEM by comparing the results with those of the exact calculations for the two-spectator-electron case. Furthermore, in UTA and STA, it has to be chosen prior to calculation whether the j-j coupled basis or LS coupled basis should be taken for the construction of radiative transition arrays. In contrast to that, the NISEM treats the transition array from first principles, which fully includes relativistic effects. Our method NISEM evaluates the x-ray spectrum of a high-Z ion with many spectator electrons using the data basis, namely, the spectra of ions with one spectator electron, which is generated by the GRASP2 code. Using the NISEM, the time for calculating the spectral profile in the many-spectator-electron case can be significantly reduced. According to the results obtained in the present paper, the UTA and STA results are found to be basically consistent with the detailed calculations and the NISEM.

In Sec. II, we investigate the basic features of the ionic system consisting of a nickel-like gold ion (Au^{51+}) plus one or two spectator electrons. We illustrate with a couple of numerical examples the line by line calculation. In Sec. III, we discuss the feasibility and effectiveness of the present plasma analysis based on an elaborate line by line atomic structure calculation. Furthermore, we introduce an extrapolation model called NISEM. In Sec. IV, we present the spectral profiles of nickel-like gold ions with many-spectator electrons under this model and the model of local thermodynamic equilibrium (LTE). Each spectrum has a broad red wing similar to the spectrum discussed by Busquet *et al.* [6]. We evaluate the electron temperature of the real plasma under a fixed electron density. Conclusions are given in Sec. V.

II. ELECTRONIC STRUCTURE OF NICKEL-LIKE GOLD IONS WITH ONE- OR TWO-SPECTATOR ELECTRON

Generally speaking, a single-electron orbital must be orthogonal to all the lower-lying orbitals with the same symmetry. Namely, we must take into account all the lower-lying orbitals in a multiconfiguration atomic structure calculation if we require the orthogonality constraint on the atomic orbitals [16]. To obtain the Rydberg orbitals of $Au^{+51}+e$ up to the principal quantum number $n=7$ and up to the azimuthal quantum number $l=n-1$, we include all the configurations composed of one of the nl orbitals with $n=5,6,7$ and $l=0,1\ldots,n-1$, and an ionic configuration $1s^2 2s^2 2p^6 3s^2 3p^6 3d^{10}$. Fortunately, we need not include an open shell ionic configuration $1s^2 2s^2 2p^6 3s^2 3p^6 3d^9 4f^1$ in the calculation. The single-electron Dirac-Fock orbitals are well defined and they are scarcely affected by the presence of such an open shell ionic configuration. We found that s and p orbitals are strongly influenced by relativistic effects even in the higher-most orbitals, whereas in others the relativistic nature is moderate. Because an electron with a lower angular momentum may come close to the atomic nucleus, the relativistic effect appears even for higher Rydberg orbitals. Examining the quantum defect, we also found that the orbital nature is well Coulombic outside the ion core. We are interested in the $3d$-$4f$ transition in the presence of one or two spectator electrons. In this transition, there is, in principle, a chance for the spectator electrons to be shaken up or down into different spectator orbitals. However, it is quite rare in the present case, because the single-electron orbitals

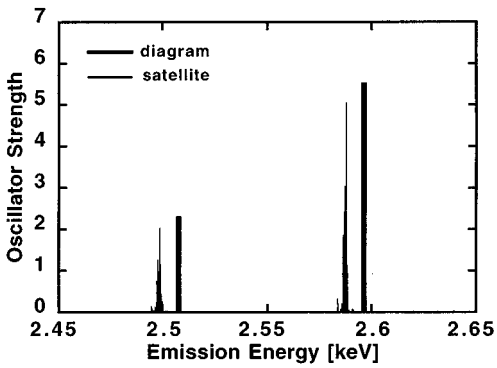

FIG. 4. Oscillator strength distribution of $5p6d$ double spectator electron satellites for transitions:
$Au^{49+}\ 1s^2 2s^2 2p^6 3s^2 3p^6 3d^9 4f^1 5p^1 6d^1$
$\rightarrow Au^{49+}\ 1s^2 2s^2 2p^6 3s^2 3p^6 3d^{10} 5p^1 6d^1$.
The $3d$-$4f$ diagram lines are also presented for comparison as thick bars.

TABLE I. Spectral parameters for $3d$-$4f$ transitions in the nickel-like gold ion using GRASP2 [14,15].

Initial J_i	Initial configuration $j(j_{3d},j_{4f})$	Final J_f	Emission energy (keV)	Wavelength (Å)	A coefficient (a.u.)
l	(5/2, 5/2)	0	2.471 712 9	5.016 126 5	$8.630\,929\,0\times10^{-7}$
l	(5/2, 7/2)	0	2.507 626 8	4.944 286 2	$5.083\,871\,4\times10^{-3}$
l	(3/2, 5/2)	0	2.596 308 2	4.775 415 5	$1.304\,308\,6\times10^{-2}$

are well defined and therefore the effect of electron correlation is small. We can regard the spectator electrons as the ''real'' spectators; they watch the $3d$-$4f$ transition with no interference. We are allowed to employ a two-state approximation for the calculation of oscillator strengths for the spectator satellite lines. Finally, we have examined the effect of electron correlation between two spectator electrons. As a whole, it has turned out that we need only two ionic states as a core state for the spectator state calculation; they are Au^{51+} $1s^22s^22p^63s^23p^63d^{10}$ and Au^{52+} $1s^22s^22p^63s^23p^63d^9$.

We calculated the oscillator strengths of the $3d$-$4f$ transitions of Au^{52+} (cobaltlike), Au^{51+} (nickel-like), Au^{50+} (copperlike), and Au^{49+} (zinclike) ions. Energy positions for each transition agree with experiment to almost three digits and also agree well with previous calculations [6]. We compared the oscillator strengths with the Coulomb gauge calculation [17], which corresponds to the velocity form calculation in the nonrelativistic terminology, and the Babushkin gauge calculation, which corresponds to the length form calculation. We found that both results agree with each other to within 10% for all the transitions.

We further made calculations for those ions with one or two spectator electrons. The spectator electrons are distributed within the range of the single-electron principal quantum number n from 5 to 7. Normally, the spectator electrons shift the spectral peak positions towards the lower energy side, because they reduce the effective nuclear charge which the $3d$ and $4f$ subshell electrons feel. The accuracy of the satellite line positions cannot be compared with experiments because the experimental spectra form a continuum due to the numerous emission lines. We expect the accuracy of the present satellite energy positions to be more or less the same as for the diagram lines.

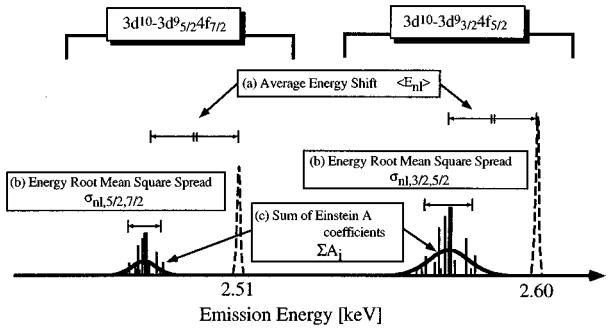

FIG. 5. Effects of the spectator electrons in $3d$-$4f$ transitions of nickel-like gold plasmas. Dashed line: Einstein A coefficients of diagram lines. Thick vertical bars: Einstein A coefficients of satellite lines. Thick Gaussian-like curve: same as the previous entry but obtained by NISEM. The NISEM curves are characterized by three parameters: (a) average energy shift, (b) energy root mean square spread, and (c) sum of Einstein A coefficients.

Figure 3 shows an example of the oscillator strength distribution for one-spectator-electron satellites corresponding to the transitions

$$\mathrm{Au}^{50+}\ 1s^22s^22p^63s^23p^63d^94f^1nd^1(n=5,6,7) \rightarrow 1s^22s^22p^63s^23p^63d^{10}nd^1, \quad (1)$$

together with the diagram lines corresponding to the transitions

$$\mathrm{Au}^{51+}\ 1s^22s^22p^63s^23p^63d^94f^1 \rightarrow 1s^22s^22p^63s^23p^63d^{10}. \quad (2)$$

Figure 4 shows an example of the oscillator strength distribution for two-spectator-electron satellites corresponding to the transitions

$$\mathrm{Au}^{49+}\ 1s^22s^22p^63s^23p^63d^94f^15p^16d^1 \rightarrow 1s^22s^22p^63s^23p^63d^{10}5p^16d^1, \quad (3)$$

together with the diagram lines.

III. APPROXIMATION METHOD FOR ANALYSIS OF X-RAY SPECTRUM OF HIGH-Z IONS WITH MANY SPECTATOR ELECTRONS

In a real plasma, we have normally a considerable population of three or more electrons in the spectator orbitals. However, the increasing number of configurations that are taken into account in the multiconfiguration Dirac-Fock calculation increases the calculation time for the line by line calculation exponentially. For example, when the number of spectator electrons increases from 1 to 3, the number of $3d$-$4f$ transitions of the nickel-like gold ion increases exponen-

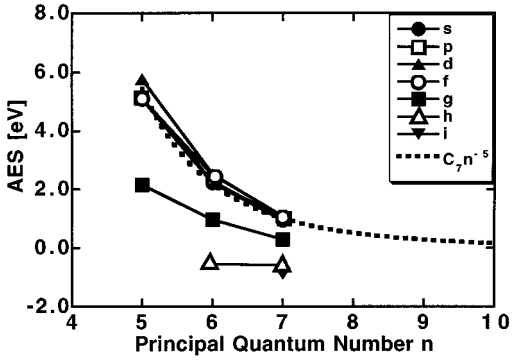

FIG. 6. Average energy shift (AES) of the $3d$-$4f$ transition for a nickel-like gold ion with one spectator electron in an nl orbital using GRASP2 [14,15]. Dashed line: AES by Eq. (7). n is the principal quantum number, and s, p, d, f, g, h, and i are the azimuthal quantum numbers.

TABLE II. Average energy shift (AES) in eV of the $3d$-$4f$ transition for nickel-like gold with one spectator electron in an nl orbital obtained using GRASP2. n is the principal quantum number, and l is the azimuthal quantum number.

$n \backslash l$	0	1	2	3	4	5	6
5	5.0940	5.1130	5.7730	5.1080	2.1540		
6	2.2130	2.2740	2.5260	2.5010	0.964 00	−0.552 00	
7	0.936 00	0.992 00	1.0430	1.0860	0.293 00	−0.588 00	−0.881 00

tially like 6×10^4, 2×10^6, and 1×10^9, respectively. Therefore, we have to explore a method to extrapolate the present result for the cases of one or two spectator electrons to the cases of three or more spectator electrons.

A. Three quantities associated with transition array

Three lines appear in $3d$-$4f$ transitions of a nickel-like gold ion (Table I). When the ion has one spectator electron, the spectral positions shift toward the lower energy side, and the number of satellite lines included in each transition array increases. However, these satellite lines are still separated into three transition arrays which are $3d^{10}$-$3d^9_{3/2}4f_{5/2}$, $3d^{10}$-$3d^9_{5/2}4f_{7/2}$, and $3d^{10}$-$3d^9_{5/2}4f_{5/2}$. Among these transitions, $3d^{10}$-$3d^9_{5/2}4f_{5/2}$ has an extremely small transition probability compared with those of the other configurations.

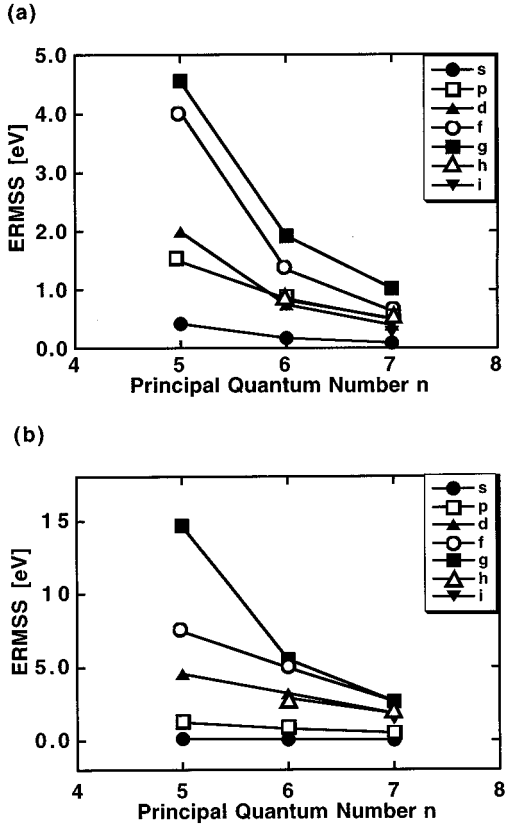

FIG. 7. (a) Energy root mean square spread (ERMSS) of the $3d^{10}$-$3d^9_{3/2}4f_{5/2}$ transitions for nickel-like gold ions with one spectator electron in the nl orbital using GRASP2. n is the principal quantum number and s, p, d, f, g, h, and i are the azimuthal quantum numbers. (b) Same as in (a) except that the transition is $3d^{10}$-$3d^9_{5/2}4f_{7/2}$.

Therefore the $3d^{10}$-$3d^9_{5/2}4f_{5/2}$ transition is neglected. If we approximate $3d^{10}$-$3d^9_{3/2}4f_{5/2}$ and $3d^{10}$-$3d^9_{5/2}4f_{7/2}$ transition arrays by two Gaussian spectra, we find that these satellite lines are described using the three quantities illustrated in Fig. 5. These are the following.

(i) The average transition energy shift from the line corresponding to the $3d$-$4f$ transition without a spectator electron, $\langle \Delta E_{nl} \rangle$, that results from a spector electron in the n,l orbit is called the AES (average energy shift). The AES is calculated by the following procedure.

The average energy of a transition array is defined by the following equation for the gold ion with no spectator electrons:

$$\langle E_0 \rangle = \frac{\sum_i A_{i0} E_{i0}}{\sum_i A_{i0}}, \tag{4}$$

where E_{i0} and A_{i0} are the ith emission energy and Einstein A coefficient, respectively. In the same way, the average energy of a transition array of the gold ion with one spectator electron is

$$\langle E_{\mathrm{spc},nl} \rangle = \frac{\sum_i A_{\mathrm{spc},nl,i} E_{\mathrm{spc},nl,i}}{\sum_i A_{\mathrm{spc},nl,i}}, \tag{5}$$

where $E_{\mathrm{spc},nl,i}$, $A_{\mathrm{spc},nl,i}$ are the emission energy and the Einstein A coefficient for the ith transition of the gold ion with

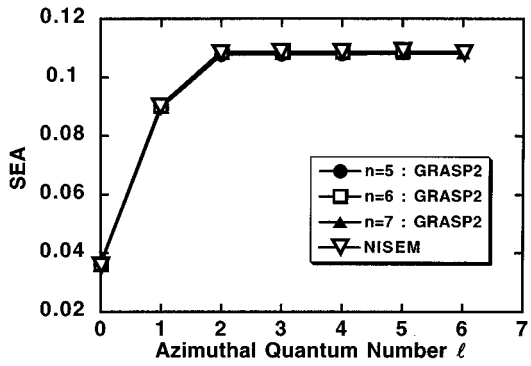

FIG. 8. Sum of Einstein A coefficients (SEA) for $3d$-$4f$ transitions of nickel-like gold ions with one spectator electron in the nl orbital using GRASP2. The notation a.u. represents atomic units. n is the principal quantum number.

TABLE III. The number of possible transitions coresponding to the $3d$-$4f$ transition for nickel-like gold ions with one spectator electron in an nl orbital. s, p, d, f, g, h, and i indicate the azimuthal quantum number.

Azimuthal quantum number l	s	p	d	f	g	h	i
The number of possible transitions N	2	5	6	6	6	6	6

a spectator electron in an nl orbital, respectively. From these average energies, we define the AES as follows:

$$\langle \Delta E_{nl} \rangle = \langle E_0 \rangle - \langle E_{\mathrm{spc},nl} \rangle. \tag{6}$$

In a real plasma, we may have a significant population of the spectator electrons in Rydberg orbitals which are higher than the highest one we can calculate with the GRASP2 code. Therefore, we made an extrapolation formula based on calculations of the AES for one spectator electron in the higher principal quantum number n states. Namely, we have examined the n dependence of the AES, the shift of the satellite emission lines from the corresponding diagram line. Using Eqs. (4), (5), and (6), we calculated the AES of $3d$-$4f$ transitions of nickel-like gold ions with one spectator electron in the orbitals of principal quantum number from 5 to 7. The results are shown in Table II. In Fig. 6, we plotted the AES of the ns, np, nd, nf, ng, nh, and ni single-spectator satellite lines. We have found that the shifts practically decrease in proportion to n^{-5} and the AES can be calculated by the following equation:

$$\langle \Delta E_{nl} \rangle = C_7 \left(\frac{n}{7} \right)^{-5}, \tag{7}$$

where C_7 is the average of AES at the $n=7$ orbital.

(ii) Energy distributions of the $3d^{10}$-$3d^9_{3/2}4f_{5/2}$ and $3d^{10}$-$3d^9_{5/2}4f_{7/2}$ transition array due to one spectator electron $\sigma_{nl}(j_{\mathrm{initial},3d}, j_{\mathrm{initial},4f})$. The energy root mean square spread (ERMSS) is calculated by the following procedure. We separate two groups from the single-spectator satellite lines. One is on the higher energy side which we call the $3d^{10}$-$3d^9_{5/2}4f_{7/2}$ group, and the other is on the lower energy side which we call the $3d^{10}$-$3d^9_{3/2}4f_{5/2}$ group. For example, the ERMSS of the $3d^{10}$-$3d^9_{3/2}4f_{5/2}$ transition array is

$$\sigma_{nl}(3/2,5/2) = \left(\frac{\sum_i A_i (E_i - E_{\mathrm{ave}})^2}{\sum_j A_i} \right)^{1/2}, \tag{8}$$

where E_{ave} is average energy of the $3d^{10}$-$3d^9_{5/2}4f_{7/2}$ group, E_1 and A_i are the ith emission energy and Einstein A coefficient, respectively. Using Eq. (8), we calculated the ERMSS of the $3d$-$4f$ transitions of nickel-like gold ions with one spectator electron in orbitals of principal quantum numbers from 5 to 7. In Figs. 7(a) and 7(b), we plotted the ERMSS of the ns, np, nd, nf, ng, nh, and ni single-spectator satellite lines. We have found that the ERMSSs decrease in proportion to an inverse power of the principal quantum number n. However, there is no clear dependence of the ERMSS on the azimuthal quantum number l.

(iii) The total transition probability. We define the total transition probability by the summation of Einstein A coefficients (SEA). The SEAs of the $3d^{10}$-$3d^9_{3/2}4f_{5/2}$ and $3d^{10}$-$3d^9_{5/2}4f_{7/2}$ transition arrays are separated from the total SEA according to the ratio of the Einstein A coefficient of $3d^{10}$-$3d^9_{3/2}4f_{5/2}$ to that of $3d^{10}$-$3d^9_{5/2}4f_{7/2}$ without spectator electrons. We calculated the SEA of the $3d$-$4f$ transitions of nickel-like gold with one spectator electron with principal quantum number values from 5 to 7. In Fig. 8, we plotted the SEA of the transitions for $5l$, $6l$, and $7l$ single-spectator satellite lines. It is known that the strength of the $3d$-$4f$ transitions are not very much influenced by the presence of the spectator electrons in the orbitals under the present consideration. On the other hand, it is found in Fig. 8 that the SEA depends apparently on the azimuthal quantum number. This is because N, the number of possible transitions for the given total angular momenta in the initial and final atomic state, depends on l. Therefore, the SEA should be proportional to this number. If we take N as this number, we can

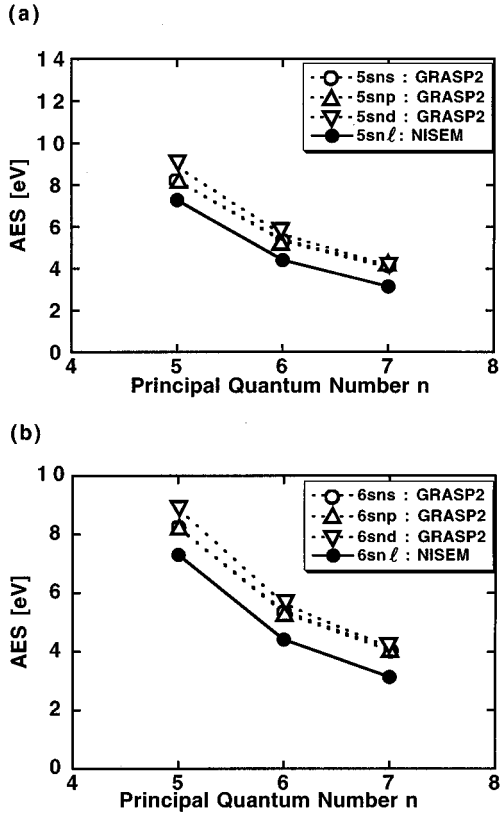

FIG. 9. (a) Comparison of AESs for $5snl$ spectator satellites by NISEM and by elaborate GRASP2 calculations. Solid lines with solid circles: NISEM. Broken lines with open circles: GRASP2 for $5sns$. Broken lines with open triangles: GRASP2 for $5snp$. Broken lines with open inverted triangle: GRASP2 for $5snd$. n is the principal quantum number. (b) Same as in (a), but for $6snl$.

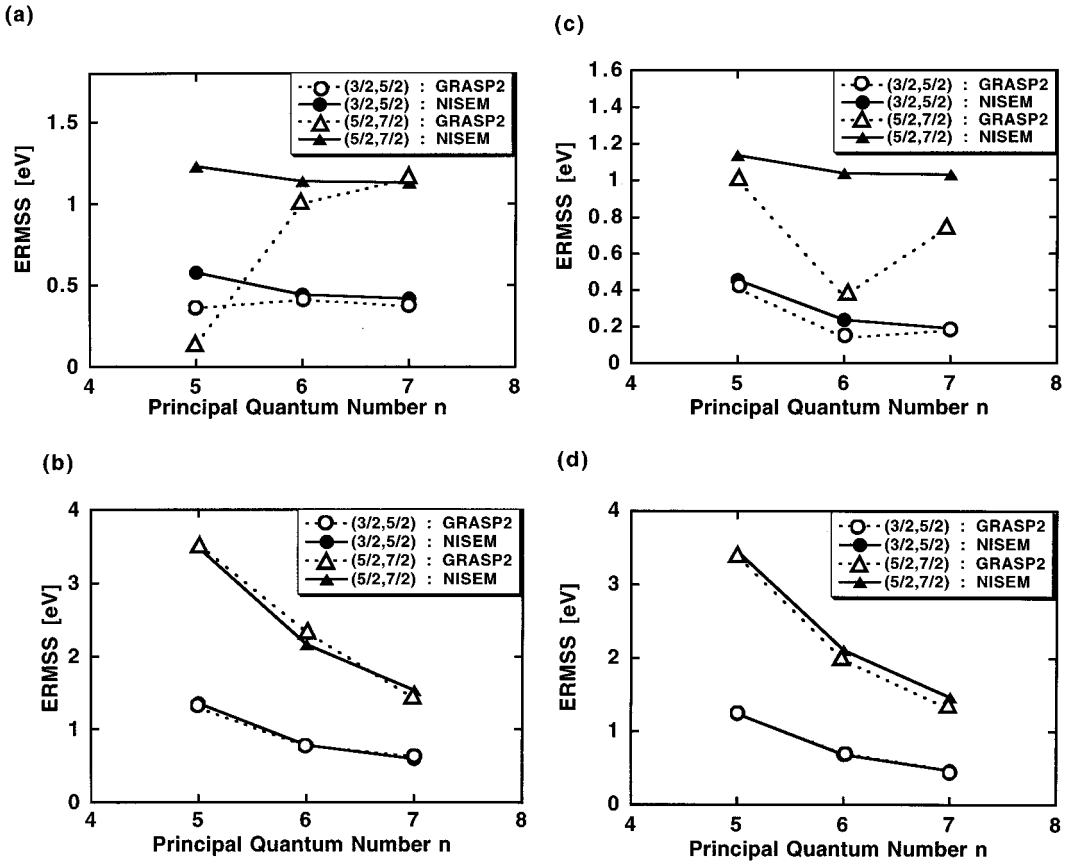

FIG. 10. (a) Comparison of the ERMSSs for $5sns$ spectator satellites by NISEM and by the GRASP2, given separately for $3d^{10}$-$3d^{9}_{3/2}4f_{5/2}$ and $3d^{10}$-$3d^{9}_{5/2}4f_{7/2}$. Broken lines with open circles: $3d^{10}$-$3d^{9}_{3/2}4f_{5/2}$ by GRASP2. Solid line with solid circles: those by NISEM. Broken lines with open triangles: ERMSSs of $3d^{10}$-$3d^{9}_{3/2}4f_{1/2}$ by GRASP2. Solid line with solid triangles: those by NISEM. (b) Same as in (a), for $5snp$ spectator satellites. (c) Same as in (a), for $6sns$ spectator satellites. (d) Same as in (a), for $6snd$ spectator satellites.

introduce the following formula for an empirical expression for the SEA:

$$\sum_i A_i = 0.01791N, \tag{9}$$

Here, 0.017 91 in the empirical formula Eq. (9) has been determined by fitting the SEA of Eq. (9) to the results of the precise numerical atomic structure calculations with GRASP2. The values of N of the $3d$-$4f$ transitions for ions with s, p, d, f, g, h, and i spectator orbitals are given in Table III.

B. Noninteracting spectator electron model (NISEM)

We introduce the NISEM in this section in order to extrapolate the results obtained by the GRASP2 calculations for the cases of one or two spectator electrons to the cases of three or more spectator electrons. As pointed out in a previous section, correlations between spectator electrons are weak in the present ionic system. In the NISEM, the correlations are neglected.

We may expect that the AES of the system with a couple of spectator electrons is the sum of AESs of the system with a single-spectator electron in the corresponding orbitals. It is also expected that the ERMSS of the many-spectator-electron system is the square root of the sum of the squares of the ERMSSs for the single-spectator-electron systems. Accordingly, we propose the following formulas:

$$\langle \Delta E_{nl,n'l',\ldots} \rangle = \langle \Delta E_{nl} \rangle + \langle \Delta E_{n'l'} \rangle + \cdots, \tag{10}$$

and

$$\sigma_{nl,n'l',\ldots} = \sqrt{\sigma_{nl}^2 + \sigma_{n'l'}^2 + \cdots}, \tag{11}$$

where $\langle \Delta E_{nl,n'l',\ldots} \rangle$ and $\sigma_{nl,n'l',\ldots}$ are the AES and ERMSS of the system with many spectator electrons in nl, $n'l'$,... orbitals. The quantities $\langle \Delta E_{nl} \rangle$ and σ_{nl} are the AES and the ERMSS with one spectator electron in the nl orbital, respectively. The third parameter SEA of the system with many spectator electrons is given by Eq. (9). In other words, we anticipate the additivity of the AES and $(\text{ERMSS})^2$ with respect to the number of spectator electrons.

Now, the formulas in Eqs. (9), (10), and (11) have been introduced by neglecting the correlations among the spectator electrons based on the observation of the characteristics of the present system, which was reviewed briefly in a previous section. However, it would still be worthy to examine the feasibility of the model NISEM by comparing the NISEM output with the results of the GRASP2 calculations. In the following, the NISEM calculations are compared with the GRASP2 calculations for the case of a nickel-like gold ion with two spectator electrons. Namely, AES, ERMSS, and

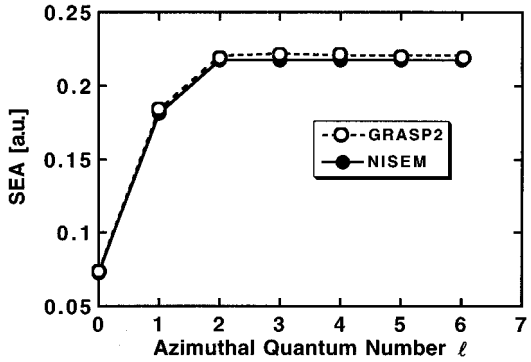

FIG. 11. Comparison of the SEAs for $5s7l$ spectator satellites by NISEM and by elaborate GRASP2 calculations. Broken line with open circles: GRASP2. Solid line with solid circles: NISEM. The notation a.u. represents atomic units.

SEA obtained by the GRASP2 code are compared with the corresponding ones from Eqs. (9), (10), and (11).

Figures 9(a) and 9(b) show the AESs for the case of two spectator electrons in the $5snl$ and $6snl$ orbitals ($l=s,p,d$). The discrepancy between the model and precise calculations is less than a few percent. Those AESs are, therefore, confirmed to be additive within an error of a few percent.

Figures 10(a), 10(b), 10(c), and 10(d) show ERMSSs for the case of two spectator electrons in the $5sns$, $5snp$, and $6sns$, orbitals with $n=5$, 6, and 7. In the cases other than $5s^2$ or $6s^2$, the agreement of Eq. (11) with the GRASP2 result is good and the discrepancy is less than a few percent. The ERMSSs can be extrapolated by using Eq. (11) within an error of a few percent. However, we can find a couple of exceptions in Figs. 10(a) and 10(c). One sees that the NISEM formula does not reproduce the ERMSS by the detailed calculation in the cases of the $5s^2$ and $6s^2$ spectator-electron configurations. The reason is that the two s electrons in the same shell form a closed shell, which has no freedom of electronic configurations to allow the statistical consideration. Consequently, Eq. (11) overestimates the data for the closed shell cases.

Figure 11 shows the SEAs for the case of two spectator electrons in the $5s$ and $7l$ orbitals. The agreement is good between Eq. (9) and precise GRASP2 calculations. The disagreement is less than a few percent.

IV. SPECTRAL PROFILE BY NISEM FOR THE SYSTEMS WITH MANY SPECTATOR ELECTRONS

In laser-produced dense plasmas, highly ionized ions may have many spectator electrons that influence the spectral profiles. By assuming a certain distribution for the population of spectator states, we can construct spectral profiles of a real plasma. Furthermore, we can determine the plasma parameters by comparing the result with experiments. Under LTE (local thermodynamic equilibrium) conditions, we calculate the spectral profiles of the $3d$-$4f$ transitions in a gold plasma in the following subsections and further make a trial to obtain a plasma temperature out of the experimental spectra [5].

A. $3d$-$4f$ transitions of nickel-like gold ions with many spectator electrons

We have calculated the emission spectra of the $3d$-$4f$ transitions from nickel-like gold plasmas in which several

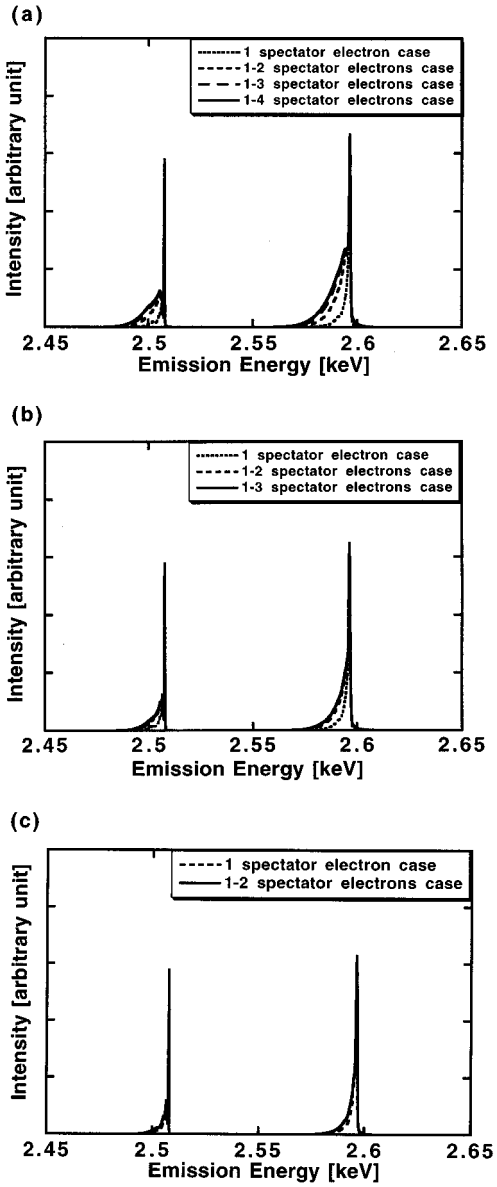

FIG. 12. (a) Spectral profile of $3d$-$4f$ transitions from nickel-like gold plasma with many spectator electrons at the electron density of 1.5×10^{23} cm^{-3} and at the electron temperature of 0.8 keV. Dotted lines include up to one spectator electron in the principal quantum number 5–7. Short broken lines include up to two spectator electrons. Long broken lines include up to three spectator electrons. Solid lines include up to four spectator electrons. (b) Same as in (a) for the electron temperature of 1.0 keV. Dotted lines, short broken lines, and solid lines are for up to one spectator electron, up to two spectator electrons, and up to three spectator electrons, respectively. (c) Same as in (a) for the electron temperature of 1.5 keV. Broken lines and solid lines are for up to one spectator electron and up to two spectator electrons, respectively.

spectator electrons are distributed in the range of principal quantum numbers 5, 6, and 7. Figures 12(a), 12(b), and 12(c) show the spectral profiles at the electron density 1.5×10^{23} cm^{-3} and the electron temperatures 0.8, 1.0, and 1.5 keV, respectively. We find that the spectral profiles with a broad red wing are produced within the framework of NISEM and LTE. In these figures, ''the one-spectator-electron case'' indicates the spectral profiles including zero to one spectator

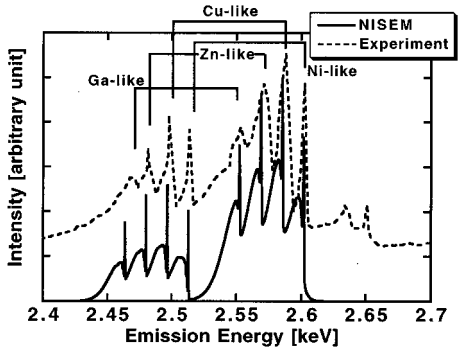

FIG. 13. NISEM spectra for the $3d$-$4f$ transition of nickel, copper, zinc, and galliumlike ions plasmas. The electron density is 1.5×10^{23} cm^{-3} and the electron temperature is 0.63 keV. Solid line represents the NISEM spectra. Broken lines represent the experimental spectra given in Ref. [5].

electron, ''the 1–2-spectator-electrons case'' indicates the spectral profiles consisting of the sum of the spectral profiles for one and two spectator electrons. Similarly ''the 1–3 spectator-electrons case,'' and ''the 1–4-spectator-electrons case'' indicate the spectral profiles consisting of the sum of the spectral profiles for 1 to 3 and 1 to 4 spectator electrons, respectively. At 0.8 keV, we find that the agreement of the spectral profiles between ''from 1 to 4'' and ''from 1 to 3'' is good. Hence, we can reproduce the real spectral profiles by taking into account up to three spectator electrons. At 1.0 keV and 1.5 keV, we only have to take into account up to two spectator electrons to reproduce the real spectral profiles.

B. Determination of plasma electron temperature

By summing up all the possible spectral profiles shown in Figs. 12, with some appropriately chosen weights, we construct nine radiation spectra that may be directly compared with one of the experiments; for example, the experimental spectra shown in the paper of Bauche-Arnoult *et al.* [5]. We adjust the theoretical spectra to the experimental ones by varying the electron temperature. We have included the $3d$-$4f$ transitions of the nickel, copper, zinc, and galliumlike gold ions. The numbers of spectator electrons considered are from 1 to 5, and their principal quantum numbers are from 5 to 7. The spectral profiles of copper, zinc, and galliumlike gold ions are obtained by shifting the spectral profile of nickel-like gold ion using Eq. (7). As for the population of these ions, we used the LTE model. Although the applicability of LTE for those ionic populations is not sure, we assume LTE as the first trial in the present paper, in order to see how the overall spectra look. The electron density is fixed at 1.5×10^{23} cm^{-3}. By varying the electron temperature, we have found that 0.63 keV for the electron temperature gives the best fit. The comparison of NISEM spectra at the best fit condition with experiments is given in Fig. 13. As found in this figure, the experimental spectra are reproduced qualitatively even in the framework of NISEM and LTE.

V. CONCLUSION

In this work, we calculated the transition energies and the oscillator strengths for many combinations of the states of nickel, copper, zinc, and galliumlike gold ions with one or two spectator electrons. *Ab initio* multiconfiguration Dirac-Fock calculations have been carried out. We have presented a method for analyzing the x-ray spectra of laser-produced gold plasmas that is called the noninteracting spectator electron model (NISEM). Using NISEM, we calculated the *M*-shell x-ray spectra for nickel-like gold ions with many spectator electrons. NISEM uses three quantities which characterize the spectrum from the ions with one spectator electron and are obtained from the results of precise detailed calculation. They are (a) average energy shift (AES), (b) energy root mean square spread (ERMSS), and (c) sum of the Einstein *A* coefficients (SEA). By the use of these three quantities for nickel-like ions, it is possible for us to calculate the spectra of ions with many spectator electrons. Because the NISEM requires the detailed calculation only for the one-spectator-electron case, the NISEM calculation time is significantly less than that of the detailed calculations. The agreement between the results of NISEM and those of the detailed calculation is very good, except for the case when two or more spectator electrons are in the same shell. In view of the degree of approximations, we can replace a fully detailed atomic structure calculation and the methods called UTA or STA by NISEM. It is found in the present study that the results of the UTA and STA are basically consistent with those of NISEM and also with the detailed calculation results, except for the accurate position of the line center.

[1] D. J. Nagel *et al.*, Phys. Rev. Lett. **33**, 743 (1979).
[2] P. G. Burkhalter, D. J. Nagel, and R. R. Whitlock, Phys. Rev. A **9**, 2331 (1974).
[3] D. L. Matthews *et al.*, J. Appl. Phys. **54**, 4260 (1983).
[4] P. Mandelbaum *et al.*, Phys. Scr. **27**, 39 (1983).
[5] C. Bauche-Arnoult *et al.*, Phys. Rev. A **33**, 791 (1986).
[6] M. Busquet *et al.*, Phys. Scr. **31**, 137 (1985).
[7] C. Bauche-Arnoult, J. Bauche, and M. Klapisch, Phys. Rev. A **20**, 2424 (1979).
[8] C. Bauche-Arnoult, J. Bauche, and M. Klapisch, Phys. Rev. A **25**, 2641 (1982).
[9] C. Bauche-Arnoult, J. Bauche, and M. Klapisch, Phys. Rev. A **30**, 3026 (1984).
[10] C. Bauche-Arnoult, J. Bauche, and M. Klapisch, Phys. Rev. A **31**, 2248 (1985).
[11] A. Bar-Shalom *et al.*, Phys. Rev. A **40**, 3183 (1989).
[12] J. Stein, D. Shalitin, and Akiva Ron, Phys. Rev. A **35**, 446 (1985).
[13] F. Koike, Nucl. Instrum. Methods **98**, 98 (1995).
[14] I. P. Grant, Adv. Phys. **6**, 747 (1970).
[15] K. G. Dyall *et al.*, Comput. Phys. Commun. **55**, 425 (1989).
[16] F. Koike, K. Honda, and K. Mima, *UV and X-Ray Spectroscopy of Astrophysical and Laboratory Plasmas*, edited by K. Yamashita and T. Watanabe, Frontiers Science Series No. 15 (Universal Academy, Tokyo, 1996), pp. 53–58.
[17] I. P. Grant, J. Phys. B **7**, 1458 (1974).